Proceedings of the ASME 2024
International Design Engineering Technical Conferences and
Computers and Information in Engineering Conference
IDETC/CIE2024
August 25-28, 2024, Washington, DC, USA

DETC2024-143184

BLUFF BODY, PIEZOELASTIC OSCILLATOR: REDUCED-ORDER MODEL, VORTEX-INDUCED VIBRATIONS, AND ENERGY HARVESTING

Andrés Bellei

Department of Mechanical Engineering, University of Maryland, College Park, MD

Balakumar Balachandran

Department of Mechanical Engineering, University of Maryland, College Park, MD

ABSTRACT

Energy harvesting from flow-induced vibrations has gained substantial attention in the last two decades due to the rising demand for renewable and sustainable energy sources, as well as the widely availability of these sources, offering a viable alternative in areas where other ambient energy sources are not accessible. Flow-induced vibrations of bluff bodies are characterized by complex nonlinear dynamics, for which accurate models are currently lacking.

In this work, a circular cylinder attached to the free end of a piezoelastic cantilever is considered for energy harvesting. When placed in a flow, this system undergoes vortex-induced vibrations. A reduced-order model is developed to understand fluid-structure interactions of this system. A wake oscillator has been used to describe vortex-induced vibrations and a finiteelement model has been used to model the piezoelastic cantilever. The developed model is used to explore the interplay amongst the fluid, structure, and piezoelectric element. The results obtained are compared to experimental data from literature, in terms of the vibration amplitude, vibration frequency, and power obtained. Modifications to the wake oscillator model are examined to better reflect the fluid-structure interactions. It is found that there is a trade-off between accurately predicting the vibration amplitude and accurately predicting the vibration frequency.

Keywords: vortex-induced vibrations, energy harvesting, reduced-order model, nonlinear oscillations

1. INTRODUCTION

In the face of climate change, clean and renewable energy sources have become crucial for a sustainable future. The prospect of harvesting clean and renewable energy from the environment is of great interest [1]. In addition, there is an

identified need for wire-free operation of sensors, and this need has been driven by factors such as the significant cost associated with power supply cables, sensors located on moving components, and sensors embedded within structures. Challenges associated with conventional battery-powered solutions include limited capacity, the need for periodic replacement, and environmental hazards [2]. This has spurred research into alternative power sources based on energy harvesting.

Kinetic energy harvesting devices have the advantage of being clean, stable, and of small size in comparison to others. Furthermore, they can be used in environments where thermal or solar energy is not available. Mechanical vibrations, a common form of kinetic energy in many systems, can be converted into electrical energy by using various mechanisms, including electromagnetic induction, piezoelectric effect, electrostatic effect, triboelectric effect, dielectric effect, and so on [3].

Among these, the piezoelectric effect has many advantages, such as having a low-cost, high-power density, simplicity, and ease of miniaturization [4]. A piezoelectric cantilever beam, a widely adopted geometry for harvesting energy from vibrations, can take the form of either a unimorph, with a single piezoelectric layer on top of the beam, or a bimorph with piezoelectric layers on both the upper and lower surfaces of the beam [3]. Related to this, it is noted that Erturk and Inman [5] developed and validated a distributed-parameter model of a piezoelectric cantilever beam subjected to harmonic excitations. Ayed et al. [6] demonstrated that the performance of a cantilever beam harvester can be improved by varying the width of the beam. In the geometries they considered, they used either a linear or a quadratic function of the axial position for the width, as the fundamental natural frequency and mode shape are strongly affected by these variations. They found that the quadratic shape can yield up to two times the energy harvested compared to that

harvested with a rectangular shape. In the aforementioned studies, base excitations are considered.

Flow-induced vibrations (FIVs) have also been studied for energy harvesting applications. FIVs are a physical phenomenon, which is associated with aerodynamic instability or vortex shedding when a fluid passes around a slender structure. The result is an oscillatory motion of the structure. These phenomena have the potential for utilization, and they can be used to harvest hydraulic energy, wind energy, and energy of a flowing gas in heating, ventilation, and air conditioning systems [7]. Examples of FIVs are vortex-induced vibrations, flutter, galloping, and wake galloping. FIVs based energy harvesting involves the coupling of three primary components, namely, fluid dynamics, structural dynamics, and electrical transduction. Often, this coupling is complex and nonlinear.

One example of a FIVs based energy harvester is a microenvironmental energy-capturing device designed to capture vibration imposed by a flow. Such a device can be used to harvest energy from the surrounding flow field to supply energy to a micro-electro-mechanical system (MEMS), wireless sensor networks, structural health monitoring systems, and so on [7].

Erturk et al. [8] used flutter of a piezoelectric airfoil to generate electrical power. They reported 10.7 mW electrical power for $100~\rm k\Omega$ resistance. In their equations, they introduced a piezoelectric coupling to the plunge degree of freedom, and they considered a load resistance in the electrical field. Bibo and Daqaq [9] considered a combined flutter-based airfoil with a base excitation harvester to increase the transduction capabilities and power density of the harvester. A higher performance for the combined loading was found. Roccia et al. [10] developed a two-dimensional computational model for predicting the aeroelastic response as well as the output power of vertically arranged airfoil harvesters. They found that the flutter speed is significantly decreased as the distance between the harvesters is reduced, which could be beneficial for effective low speed energy extraction.

Vortex-induced vibrations (VIVs) are another example of FIVs, and the associated characteristic synchronization region has attracted much attention for energy harvesting. This phenomenon occurs when a sufficiently bluff body is exposed to a fluid flow and vortex shedding occurs in the wake of the body at or near a structural natural frequency of the body. As the flow speed increases, a critical point is reached when the vortex formation frequency is close enough to the body's natural frequency, resulting in unsteady pressures from the wake vortices that induce a response from the body [11].

Akaydin *et al.* [12] introduced a self-excited piezoelectric fluid harvester based on VIVs. Through their results, they showed a maximum of 0.1 mW non-rectified electrical power that was achieved for a flow speed of about 1.19 m/s. Dai *et al.* [13] investigated the effect of the orientation of the bluff body attached to the cantilever beam in the synchronization region. They found that the orientation should be different for different wind speed regions. In particular, for low wind speeds of $\sim 1.3 - 1.8$ m/s, they suggested that the bluff body should be aligned with the beam. In wind tunnel experiments, Azadeh-Ranjbar *et*

al. [14] studied the unsteady responses for different aspect ratios (defined as the ratio of the length of the cylinder to the cylinder's diameter) of finite length rigid circular cylinders with spanwise free-ends undergoing VIVs. They found that as the aspect ratio is decreased from 28.8 to 5.0, there is an unexpected 200% broadening of the lock-in region and an almost 230% increase in the peak oscillation amplitude.

To understand the fundamental physics of VIVs, the classical reference is an elastically mounted rigid circular cylinder restrained to move transverse to the flow. In a landmark study conducted in 1968, Feng outlined relationships between the amplitude and frequency of the fluid forcing as a function of the system parameters and the flow speed [15]. Two essential features are observed: a large oscillatory motion in a limited range of fluid speed, and simultaneously, a significant change in the frequency. With regard to the frequency response, a phenomenon called lock-in or synchronization was found to occur. The classical definition of lock-in phenomenon corresponds to the situation wherein the oscillation frequency (f), as well as the vortex formation frequency (f_{vs}) , are close to the natural frequency (f_N) of the structure throughout the regime of large-amplitude vibrations, so that $f^* = f/f_N \sim 1$.

As VIVs represent a complex nonlinear phenomenon, phenomenological models have been considered. These models have several attractive attributes, including the following: they offer a simplified representation of complex behavior, helping capture the essential dynamic characteristics and providing a means to obtain approximate solutions and predictions [16]. Currently, the wake oscillator model is a well-accepted model for studying vortex-induced vibrations. The original idea of using a wake oscillator equation was proposed by Bishop and Hassan in 1964 [17], and later modified in the work of Hartlen and Currie in 1970 [18]. The model consists of a coupled two-degree of freedom system: the cylinder and the wake. More recently, Facchinetti et al. [19] proposed using the van der Pol equation for the wake variable and a coupling term proportional to the acceleration of the cylinder. The proposed equations for this model are presented in detail in Section 2.1.

2. MATERIALS AND METHODS

Here, the authors' aim is to model vortex-induced vibrations (VIVs) of a circular cylinder attached to a cantilever beam with a piezoelectric patch transducer and estimate the amplitude of vibrations, the associated frequency content, and the power which can be harvested from the system. First, the wake oscillator model, which is adopted for describing VIVs, is presented in Section 2.1. A finite element model is developed to describe the cantilever beam with a piezoelectric patch and the attached circular cylinder. This configuration is further described in Section 2.2. A combination of both models is derived and presented in Section 2.3 to describe the dynamics of the VIV energy harvester. Although finite element models for bluff bodies attached to cantilevers have been developed (e.g., [20]), to the best of the authors' knowledge, the development considered here has not been used for an energy harvester, as in most studies, only lumped parameter models are considered.

2.1. Wake Oscillator Model

As discussed earlier, the wake oscillator model is currently a well-accepted model for studying VIVs of an elastically supported rigid circular cylinder. As proposed by Facchinetti *et al.* [19], the structure is described by a single degree-of-freedom linear oscillator. The fluctuating nature of the vortex street is modelled by a nonlinear oscillator, the van der Pol oscillator, herein referred to as the wake oscillator. In dimensional form, the coupled wake and structural oscillators are described by the system

$$\left(m_s + \frac{\pi C_M \rho D^2}{4}\right) \ddot{y} + (c_s + 2\pi \gamma \rho \text{St}UD) \dot{y} + k_s y$$

$$= \frac{\rho U^2 D C_{LO}}{4} q \qquad (1)$$

$$\ddot{q} + \varepsilon \left(\frac{2\pi \text{St}U}{D}\right) (q^2 - 1) \dot{q} + \left(\frac{2\pi \text{St}U}{D}\right)^2 q = \frac{A}{D} \ddot{y}$$

where y and q are the two degrees of freedom of the system, associated with the in-plane cross-flow displacement of the structure and the lift coefficient for the structure, respectively. The rest of the parameters are the cylinder's mass m_s , a mass coefficient C_M , which is 1 for circular cross sections, air density ρ , cylinder's diameter D, viscous dissipation of support c_s , Strouhal number St, free stream velocity of the uniform flow U, stiffness of the structure k_s , reference lift coefficient observed on a fixed structure subjected to vortex shedding C_{LO} , and fluid added damping coefficient γ that is directly related to the mean sectional drag coefficient C_D of the structure through $\gamma =$ $C_D/4\pi$ St. The coefficients ε and A need to be obtained from experimental results. Facchinetti et al. [19] estimated these parameters by analyzing the effects of an imposed motion of the structure on the near wake dynamics at resonance, and thus also assuming a harmonic motion in that state. Building on this, Xu et al. [21] also considered a harmonic motion but estimated different parameters for the region before resonance and the region after resonance, leading to a better estimation of the amplitude of vibration.

2.2. Finite Element Model

The finite element model is based on the work of Beltramo et al. [22], who introduced a model of a strain-based geometrically nonlinear piezoelectric beam for modeling energy harvesters. Elementary beam theory is used, following the Euler Bernoulli beam theory. A linear two-node element is adopted in this work, with each node having two degrees of freedom: one translation degree of freedom u and one rotation degree of freedom θ . In addition to the structural part, the piezoelectric layer must be considered. To that end, one or two piezoceramic layers can be utilized to cover the upper, lower, or both surfaces of the elastic substrate. The electrodes of the piezoelectric layers are assumed to be perfectly conductive, and their thickness values are assumed to be negligible. When modeling a bimorph piezoelectric beam, comprising two piezoceramic layers, the electrodes of both layers are connected in series. A resistive load

R is included in the circuit to dissipate energy. The governing equations of the coupled system are given by

$$\mathbf{M}\ddot{\mathbf{y}} + \mathbf{C}\dot{\mathbf{y}} + \mathbf{K}\mathbf{y} + \mathbf{\Theta}v_e = \mathbf{F}(t)$$
$$-\mathbf{\Theta}^T\dot{\mathbf{y}} + C\dot{v}_e + \frac{v_e}{R} = 0$$
(2)

where **M** is the global mass matrix, **K** is the global stiffness matrix, **O** is the linear electromechanical coupling vector, C and R are the capacitance and resistance of the electric circuit, respectively, and v_e is the generalized electric coordinate.

Regarding the attachment of the cylinder of diameter D at the free end of the beam (x = L), it is treated as a point mass located at a distance D/2 from the last node at the free end of the beam, with its mass moment of inertia considered. Thus, the kinetic energy of the cylinder is expressed as

$$T = \frac{1}{2} m_t \left[\frac{\partial u(x,t)}{\partial t} \bigg|_{x=L} + \frac{D}{2} \frac{\partial \theta(x,t)}{\partial t} \bigg|_{x=L} \right]^2 + \frac{1}{2} I \left[\frac{D}{2} \frac{\partial \theta(x,t)}{\partial t} \bigg|_{x=L} \right]^2$$
(3)

where m_t is the mass of the cylinder and the moment of inertia, given by $I = I_G + m_t \left(\frac{D}{2}\right)^2$, is considered from the surface of the cylinder where it is attached to beam.

2.3. Combined Reduced-Order Model

The models previously described are combined to obtain the reduced-order model of the energy harvester. To that end, it is assumed that the fluid-structure interaction occurs only through the wake and the cylinder. The resulting combined system of equations of the model reads as follows:

$$\mathbf{M}_{\mathbf{coupled}} \ddot{\mathbf{y}} + \mathbf{C}_{\mathbf{coupled}} \dot{\mathbf{y}} + \mathbf{K} \mathbf{y} + \mathbf{\Theta} v_e = \mathbf{F} q$$

$$-\mathbf{\Theta}^T \dot{\mathbf{y}} + C \dot{v}_e + \frac{v_e}{R} = 0$$

$$\ddot{q} + \varepsilon \left(\frac{2\pi \mathrm{St} U}{D}\right) (q^2 - 1) \dot{q} + \left(\frac{2\pi \mathrm{St} U}{D}\right)^2 q$$

$$= \frac{A}{D} (\ddot{y}_{N-1} + \frac{D}{2} \ddot{y}_N)$$
(4)

where $\mathbf{M_{coupled}}$ is the global mass matrix modified to include the added mass of the cylinder, $\mathbf{C_{coupled}}$ is the global damping matrix modified to include the fluid damping, and \mathbf{F} is a null vector except at the coordinates N-1 and N, which correspond to the displacement of the cylinder, where it takes the value $\frac{\rho U^2 D C_{LO}}{4}$ and $\frac{\rho U^2 D C_{LO}}{4}$, respectively.

3. RESULTS AND DISCUSSION

Numerical simulations are carried out and the obtained results are compared to those obtained from various

experimental studies, in all of which a circular cylinder has been attached to the free end of a cantilever beam. The beam consists of an aluminum shim with a piezoelectric patch and a strain gauge bonded near the clamped end, as shown in Figure 1, which corresponds to the one used by Azadeh-Ranjbar *et al.* [14].

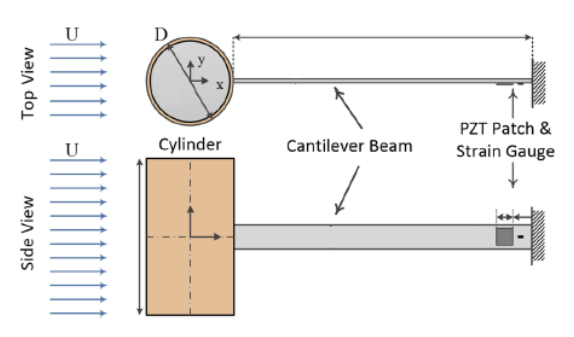


Figure 1: Schematic view of the experimental energy harvester from Azadeh-Ranjbar *et al.* [14]. The system consists of a circular cylinder mounted on the upstream tip of a cantilever beam. the piezoelectric (pzt) patch and the strain gauge are located close to the beam's fixed end.

In all of the experiments compared, a voltage signal is measured from the strain gauge and then converted into displacement or power through appropriate relationships. By contrast, with the developed model, both the displacement of the system and the voltage produced from the piezoelectric patches can be obtained. Thus, by conducting simulations with the model, one can obtain a more complete picture of the dynamics of the different variables involved and the coupling effects, than what was possible in the previously conducted experiments. Furthermore, in the available experimental data, only one of the following variables is available: i) the vertical displacement of the cylinder, ii) voltage produced from the strain gauge, and iii) calculated power produced. Hence, different comparisons are made here.

3.1. Amplitude and frequency of vibration

The amplitude and frequency of vibration are calculated for the considered energy harvester, following the work reported by Azadeh-Ranjbar *et al.* [14]. The main geometric and mechanical properties of the system are presented in Table 1. In this study, the authors explore different aspect-ratios of cylinders (defined as the ratio of the length of the cylinder to the cylinder's diameter) to investigate the effects on VIVs and the dynamic response of the system. In the present studies, the highest aspect-ratio considered is 28.

The choice of what Strouhal number to use in the considered model is not obvious. In the wake oscillator model, it is common practice to assume St = 0.200, which corresponds to the Strouhal number in the sub-critical range for a stationary cylinder. Azadeh-Ranjbar *et al.* [14] reported a St number of 0.178 outside the lock-in region. With the choice of this number, the frequency of oscillation of the structure is well reproduced by the model, as can be noted from Figure 2. Another possible choice is to use the value of the Strouhal number at the peak of the amplitude response curve inside the lock-in region, as was

Table 1: Properties of the energy harvester from Azadeh-Ranjbar *et al.* [14]

Physical properties	PZT	Beam	Cylinder
	element		
Length [mm]	23.5	160	604.8
Width [mm]	23.5	32.5	-
Thickness [mm]	0.267	0.635	-
Diameter [mm]	-	-	21
Mass density [kg/m ³]	7800	2730	-
Mass [g]	1.6	9	28.8
Young's modulus [GPa]	52	73	_
Strain coefficient [pm/V]	-190	-	-
Permittivity at constant	15.66	-	-
strain [nF/m]			
Capacitance [nF]	39	-	-

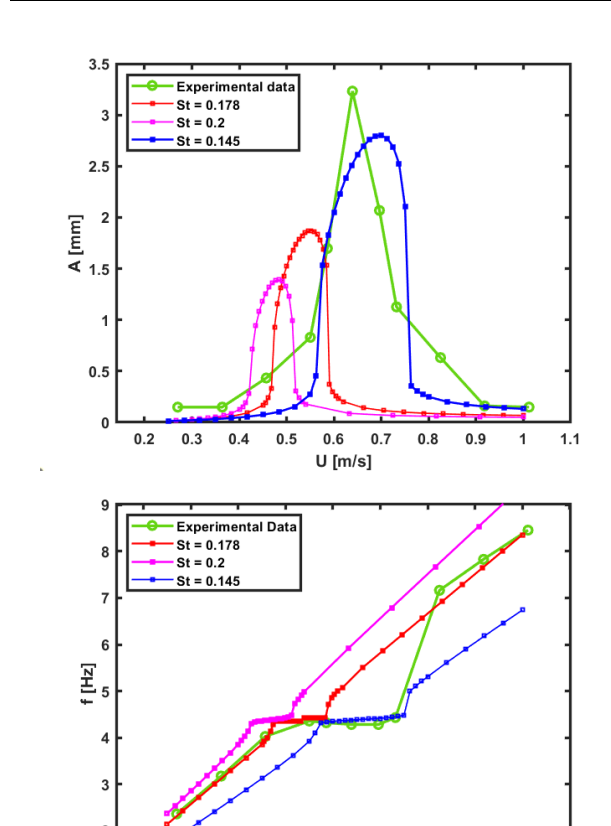


Figure 2: Vortex-induced vibration response of a circular cylinder attached to a cantilever beam. Comparisons of the amplitude of vibration and the frequency of vibration as a function of the freestream speed with Facchinetti *et al.*'s model [19] for different Strouhal numbers. Comparisons are made with Azadeh-Ranjbar *et al.*'s [14] experimental results.

0.6 0.7 0.8 0.9

done by Dai *et al.* [23]. For the considered experiments of Azadeh-Ranjbar *et al.* [14], this value turns out to be St = 0.145. The three possibilities are explored by using Facchinetti *et al.*'s model [19] for the wake variable, and the obtained simulation

results are presented in Figure 2 along with the experimental results.

From the amplitude plot on top, by using the Strouhal number at the peak of the lock-in region (blue curve), one obtains a more accurate response curve, both in terms of amplitude magnitude and location of the curve as a function of wind speed, whereas with a Strouhal number of 0.200, one obtains a curve that is the least accurate. By contrast, upon comparing the curves in the frequency plot shown in the bottom, with the curve in red that corresponds to a Strouhal number outside lock-in region, one appears to better capture the experimental results. For this case, the model results are seen to follow the same slope as obtained for the experimental results, both outside the lock-in region as well as inside. However, since the lock-in region and peak amplitudes of vibration occur at lower speeds (top plot), for the curve in red in the frequency plot, there is a lock-in region (horizontal portion) at a lower speed than that observed with the experimental results. In addition, for the curve in blue, one can see a wider lock-in region, which is closer to the experimental results. However, outside the lock-in region, the model results are found to have a different slope compared to experiments.

Another set of comparisons is presented in Figure 3; this time, with comparisons of the results obtained with the model by Facchinetti et al. [19] (red curve) and the modified model by Xu et al. [21] (blue curve). For these simulations, a Strouhal number of 0.178 is used, which corresponds to the measured Strouhal number outside the lock-in region. With Xu et al.'s model, one predicts a much better peak amplitude of vibration. The frequency of vibration outside the lock in region is well characterized by both models, and inside the lock-in region, results from both models are found to deviate from the Strouhal law, as expected and confirmed by the experimental results. However, with Xu et al.'s model, one obtains an even narrower lock-in region than that obtained with Facchinetti et al.'s model. With the modified model by Xu et al., one is also not successful in predicting the wind speed at which the peak amplitude of vibration occurs. Furthermore, this speed is underestimated.

3.2. Power produced

For the power produced by the cantilever beam with the cylinder attached at the free end, the model results are compared to those presented in the study of Akaydin *et al.* [12]. The experimental set up is similar to the previous one reported in [14], and the corresponding properties are shown in Table 2. In this case, the aspect-ratio of the circular cylinder is 5.3. Hence, spanwise free ends effects are expected to be prominent. However, these effects are not considered in the developed reduced-order model.

As with the first comparison, different Strouhal numbers are explored with Facchinetti *et al.*'s model [19]. Interestingly enough, Akaydin *et al.* [12] report a different Strouhal number at resonance; that is, 0.105, which is significantly smaller than the one reported by Azadeh-Ranjbar *et al.* [14] at resonance; that is 0.145. It is noted that the Strouhal number at resonance for the cylinder of aspect-ratio 5 is not reported in Azadeh's work. In Figure 4, the results of the simulations are shown along with the

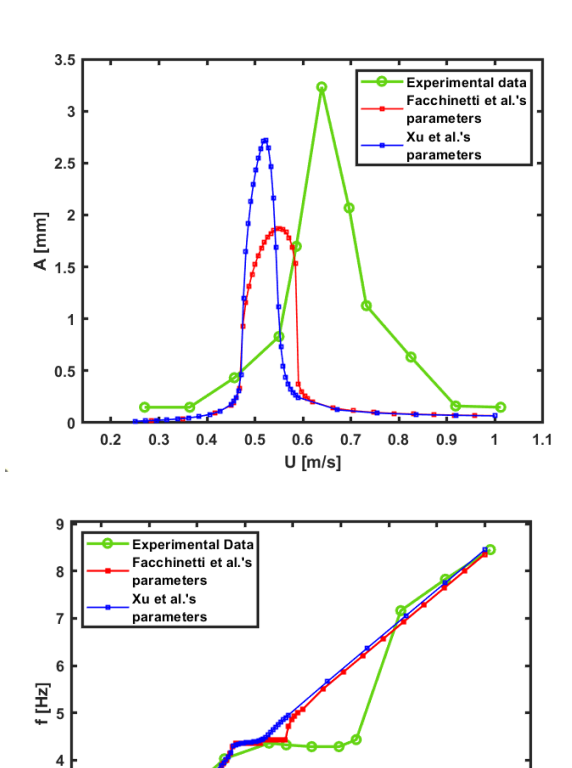


Figure 3: Vortex-induced vibration response of a circular cylinder attached to a cantilever beam. comparisons of the amplitude and frequency of vibration as a function of the freestream speed using Facchinetti *et al.*'s model [19] and Xu *et al.*'s proposed new model [21] for the wake oscillator part of the model. comparisons are made with Azadeh-Ranjbar *et al.*'s [14] experimental results. the green diagonal line is used to show the frequency predicted by using the Strouhal law for St=0.178.

0.6 U [m/s]

0.3

experimental results. Compared to Figure 2, additional curves have been added: first, results (the yellow curve) have been added by using the following parameters from Dai *et al.* [23]: A = 12, $\epsilon = 0.24$, and St = 0.116. Second, results (the magenta curve) with Facchinetti *et al.*'s [19] original parameters but with St = 0.116, in order to be able to assess the effect of the change in parameters used in reference [23] without the effect of changing the Strouhal number.

In agreement with the previous results, when the Strouhal number equal to 0.178 is used (red curve), the model results are found to provide an underestimate for the power produced by the energy harvester, and one does not capture the wind speed at which resonance occurs. A closer estimation of the power generated is achieved by choosing St = 0.145. With the Strouhal number St = 0.116, one overestimates the power produced to be almost double that of the experimental values. This is also true when one uses the reported Strouhal number at resonance, which is not shown in the plot as the trend with increasing Strouhal

number is clear. It is not clear to the authors how Dai *et al.* 's [23] results matched the experimental results so closely.

Table 2: Properties of the energy harvester by Akaydin *et al.* [12]

Physical properties	PZT	Beam	Cylinder
	element		
Length [mm]	31.8	267	210
Width [mm]	12.7	32.5	-
Thickness [mm]	0.267	0.635	-
Diameter [mm]	-	-	39.6
Mass density [kg/m ³]	7800	2730	-
Mass [g]	2	15	16
Young's modulus [GPa]	66	73	-
Strain coefficient [pm/V]	-190	-	-
Permittivity at constant	13.28	-	-
strain [nF/m]			
Capacitance [nF]	20.1	-	-

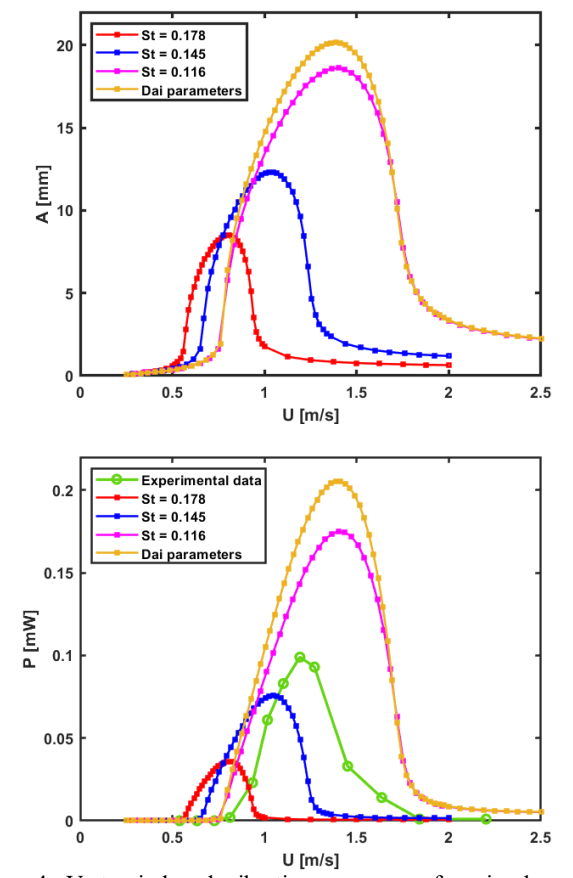


Figure 4: Vortex-induced vibration response of a circular cylinder attached to a cantilever beam. comparisons of the amplitude of vibration and the harvested power obtained by using Facchinetti *et al.*'s model [19] for different Strouhal numbers, and Dai *et al.*'s [23] proposed parameters for the wake oscillator model, with Akaydin *et al.*'s experimental results [12].

3.3. Modifications to the original wake oscillator model

To improve the model, two modifications to the classical wake oscillator model used by Facchinetti *et al.* [19] have been explored:

Through the first one, the author addresses the fact that in the original model, the Strouhal number is taken as constant, when in fact, from experiments, it is known that it is only constant outside the lock-in region, while inside the lock-in region it is the vortex shedding frequency that remains constant and equal to the structural first natural frequency of the system. The Strouhal number decreases as the wind speed increases. To implement this in the model, a lock-in region must be prescribed, and in this case, it is based on experimental results. This is a limitation for prediction purposes, as one needs to have a prior knowledge of the actual response. However, this can lead to a deeper understanding of the underlying physics of this phenomenon.

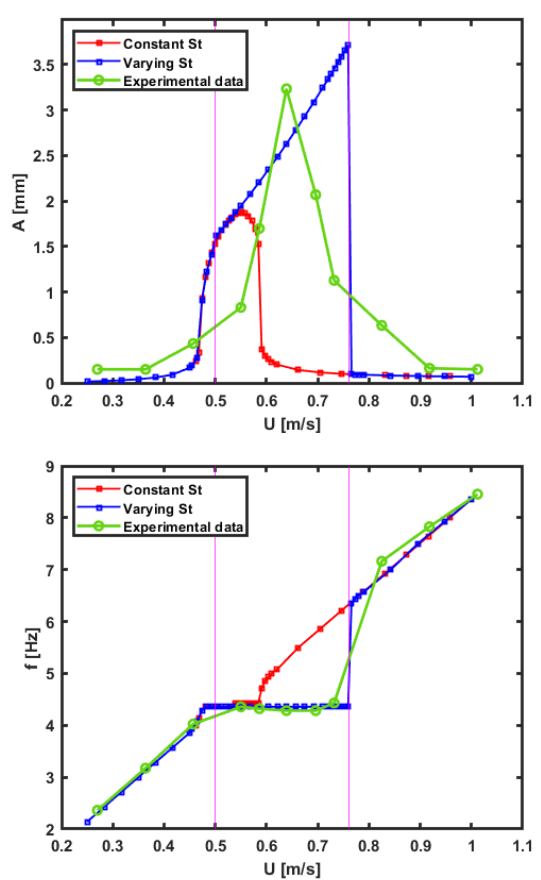


Figure 5: Vortex-induced vibration response. Comparison between results obtained with Facchinetti *et al.*'s model [19] (red curve) and the same model with a varying Strouhal number in the lock-in region.

In Figure 5 the results of this modification are shown (blue curve) and compared to the experimental results from [14] and the original model. From the results inside the lock-in region (shown by the vertical pink lines), the amplitude of vibration grows almost linearly as the wind speed is increased, which

clearly deviates from the experimental results and the original model. However, the frequency of oscillation of the system is captured much better compared than with the original model, as can be seen in the bottom plot.

Through the second modification, the authors consider a more accurate mean sectional drag coefficient C_D , which directly affects the fluid-added damping term that is a critical term in the wake oscillator model. The average drag on a vibrating cylinder at or near vortex shedding frequency increases with the transverse vibration amplitude. To capture this nonlinear behavior, a drag magnification term, expressed as $C_D = (1 + 1)^{-1}$ $2.1y/D)C_{DO}$ is considered, as proposed by Blevins [24]. The drag coefficient C_{DO} for a stationary cylinder is reported as a function of Reynolds number also in Blevins [24], and a value of 1.2 is assumed here. In Figure 6, the results obtained with this modification are compared to the experimental results and those obtained with the original model. The amplitude of vibration in the lock-in region is found to be higher compared to that from the original model. However, the lock-in region is practically the same as in the original model. Hence, for the considered case, no significant improvement to the results with the original model is found.

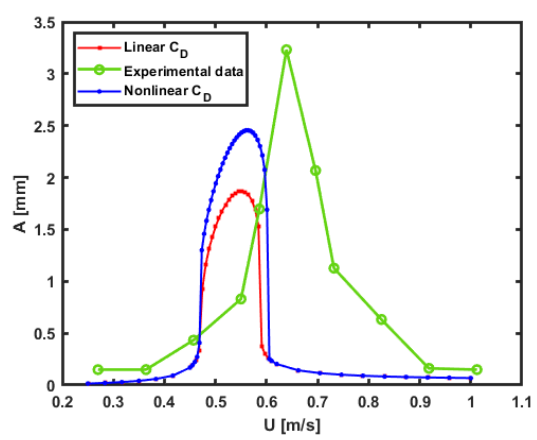


Figure 6: Vortex-induced vibration response. comparison of the results for the amplitude of vibration obtained from Facchinetti *et al.*'s original model [19] (red curve) and the same model with a nonlinear drag coefficient (blue curve).

4. CONCLUSION

A nonlinear reduced-order model is developed for energy harvesting using a piezoelectric cantilever with a circular cylinder attached to the free end. When placed in a flow, this system undergoes vortex-induced vibrations. To model the piezoelastic cantilever, a finite element model is developed. This model is coupled to a wake oscillator model, which is used to describe the vortex-induced excitation experienced by the cylinder.

To assess the model's fidelity, multiple comparisons are made with experimental data. It is found that there is a trade-off between accurately predicting the amplitude of vibration and accurately predicting the frequency of vibration. In future work, the authors plan to extend this model to multiple oscillators in different configurations and explore the associated nonlinear dynamics.

ACKNOWLEDGEMENTS

The authors gratefully acknowledge the support of the National Science Foundation through Grant No. CMMI 2131594.

REFERENCES

- [1] V. V. Quaschning, Renewable Energy and Climate Change, 2 ed., Wiley, 2020.
- [2] R. Bogue, "Energy harvesting and wireless sensors: a review of recent developments," *Sensor Review*, vol. 29, no. 3, pp. 194-199, 2009.
- [3] A. Khaligh, P. Zeng and C. Zheng, "Kinetic Energy Harvesting Using Piezoelectric and Electromagnetic Technologies State of the Art," *IEEE Transactions on Industrial Electronics*, vol. 57, no. 3, pp. 850-860, 2010.
- [4] X. Ma and S. Zhou, "A review of flow-induced vibration energy harvesters," *Energy Conversion and Management*, 2022.
- [5] A. Erturk and D. J. Inman, "An experimentally validated bimorph cantilever model for piezoelectric energy harvesting from base excitations," *Smart Materials and Structures*, 2009.
- [6] S. B. Ayed, A. Abdelkefi, F. Najar and M. R. Hajj, "Design and performance of variable-shaped piezoelectric energy harvesters," *Intelligent Material Systems and Structures*, vol. 25, pp. 174-186, 2014.
- [7] J. Wang , L. Geng, L. Ding, H. Zhu and Y. Daniil, "The state-of-the-art review on energy harvesting from flowinduced vibrations," *Applied Energy*, 2020.
- [8] A. Erturk, W. G. R. Vieira, C. J. De Marqui and D. J. Inman, "On the energy harvesting potential of piezoaeroelastic systems," *Applied Physics Letters*, vol. 96, no. 18, 2010.
- [9] A. Bibo and M. F. Daqaq, "Investigation of concurrent energy harvesting from ambient vibrations and wind using

- a single piezoelectric generator," *Applied Physics Letters*, vol. 102, no. 24, 2013.
- [10] B. A. Roccia, M. L. Verstraete, L. R. Ceballos, B. Balachandran and S. Preidikman, "Computational study on aerodynamically coupled piezoelectric harvesters," *Journal of Intelligent Material Systems and Structures*, vol. 31, no. 13, pp. 1-16, 2020.
- [11] C. Williamson and R. Govardhan, "Vortex Induced Vibrations," *Annual Review Fluid Mechanics*, vol. 36, pp. 413-455, 2004.
- [12] H. D. Akaydin, N. Elvin and Y. Andreopoulos, "The performance of a self-excited fluidic energy harvester," *Smart Materials and Structures*, 2012.
- [13] H. L. Dai, A. Abdelkefi, Y. Yang and L. Wang, "Orientation of bluff body for designing efficient energy harvesters from vortex-induced vibrations," *Applied Physics Letters*, vol. 108, no. 5, 2016.
- [14] V. Azadeh-Ranjbar, N. Elvin and Y. Andreopoulos, "Vortex-induced vibration of finite-length circular cylinders with spanwise free-ends: Broadening the lock-in envelope," *Physics of Fluids*, 2018.
- [15] C. C. Feng, "The measurement of vortex induced effects in flow past stationary and oscillating circular and d-section cylinders," The University of British Columbia, Vancouver, 1968.
- [16] M. P. Païdoussis, S. J. Price and E. de Langre, Cross flow induced instabilities, New York: Cambridge University Press, 2011.
- [17] R. E. D. Bishop and A. Y. Hassan, "The lift and drag forces on a circular cylinder oscillating in a flowing fluid," Proceedings of the Royal Society of London. Series A, Mathematical and Physical Sciencies, vol. 277, pp. 51-75, 1964.
- [18] R. T. Hartlen and I. G. Currie, "Lift-oscillator model of vortex-induced vibration," *ASCE Journal of the Engineering Mechanics Division*, vol. 96, pp. 577-591, 1970.
- [19] M. Facchinetti, E. d. Langre and F. Biolley, "Coupling of structure and wake oscillators in vortex-induced vibrations," *Fluids and Structures*, p. 123–140, 2004.

- [20] K. Z. Wani, M. Pandey and B. Balachandran, "Coupled Bluff Body Energy Harvesters: Vortex Influenced Dynamics," in *Proceedings of the IUTAM Symposium on Nonlinear dynamics for design of mechanical systems across different length/time scales*, Tsukuba, Japan, 2023.
- [21] W.-h. XU, Y.-x. WU, X.-h. ZENG, X.-f. ZHONG and J.-x. YU, "A new wake oscillator model for predicting vortex induced vibration of a circular cylinder," *Hydrodynamics*, pp. 381-386, 2010.
- [22] E. Beltramo, B. Balachandran and S. Preidikman, "Three-dimensional formulation of a strain-based geometrically nonlinear piezoelectric beam for energy harvesting," *Intelligent Material Systems and Structures*, vol. 32, pp. 2153-2173, 2021.
- [23] H. Dai, A. Abdelkefi and L. Wang, "Theoretical modeling and nonlinear analysis of piezoelectric energy harvesting from vortex-induced vibrations," *Intelligent Material Systems and Structures*, pp. 1861-1874, 2014.
- [24] R. D. Blevins, Flow-Induced Vibration, Second Edition ed., New York: Van Nostrand Reinhold, 1990.